

D₁-44
N86-26680 P-20

EFFECTS OF IMPURITIES ON SILICON SOLAR-CELL PERFORMANCE 8674

R. H. Hopkins
Westinghouse R&D Center
Pittsburgh, PA 15235

WW316529

ABSTRACT

Model analyses indicate that sophisticated solar cell designs including, e.g., back surface fields, optical reflectors, surface passivation, and double layer antireflective coatings can produce devices with conversion efficiencies above 20% (AM1). To realize this potential, the quality of the silicon from which the cells are made must be improved; and these excellent electrical properties must be maintained during device processing.

As the cell efficiency rises, the sensitivity to trace contaminants also increases. For example, the threshold Ti impurity concentration at which cell performance degrades is more than an order of magnitude lower for an 18% cell than for a 16% cell. Similar behavior occurs for numerous other metal species which introduce deep level traps that stimulate the recombination of photogenerated carriers in silicon.

Purification via crystal growth in conjunction with gettering steps to preserve the large diffusion length of the as-grown material can lead to the production of devices with efficiencies above 18%, as we have verified experimentally.

1. INTRODUCTION

For photovoltaic (PV) power generation to compete on a large scale with other forms of energy production, the price of solar cell modules must be substantially reduced. Because area-related costs, such as land, support structures, encapsulation, etc., become significant in large systems, it is now recognized that reduced system costs require much more efficient modules and cells than are currently manufactured.^(1,2)

For this reason, a major thrust of recent photovoltaic research has been to raise solar cell efficiency by innovative cell design and careful device processing coupled with improvements in the quality of the silicon material from which the cells are made. In this paper, some basic considerations for cell efficiency improvement are examined, the performance-limiting mechanisms due to impurities are described, and techniques to minimize impurity effects are outlined.

PRECEDING PAGE BLANK NOT FILMED

2. APPROACHES TO CELL EFFICIENCY IMPROVEMENT

When light shines on a solar cell, photogenerated carriers (hole-electron pairs) are produced which diffuse to, and are separated by, the high field region at the junction of the device. A photovoltage is produced, and a current flows in the external circuit connected to the cell⁽³⁻⁵⁾. If the carriers recombine before reaching the junction, they do not contribute to voltage and current; and cell efficiency is reduced. Thus the carrier diffusion length L or the recombination lifetime τ to which it is related ($L = \sqrt{D\tau}$ where D is the carrier diffusivity) must be made as large as possible. For example, L should be at least equal to the cell thickness, to maximize efficiency.

Diffusion length is a strong function of impurities and defects in the silicon which act as centers for recombination. In addition, carrier recombination at surfaces and in the heavily doped regions of the cell can also limit performance. By controlling these performance limiting factors, we increase solar cell efficiency which is given by

$$\eta = \frac{V_{oc} \times I_{sc} \times FF}{P_{IN}} \quad (1)$$

where: V_{oc} is the open circuit cell voltage

I_{sc} is the short circuit current

FF is a curve ideality factor, and

P_{IN} is the incident solar power.

Advanced cell designs and increases in the quality of the silicon material are the two main methods to improve solar cell efficiency. Such features as oxide passivation to reduce carrier recombination at surfaces, double layer antireflection coatings, back surface reflectors, back surface fields, and improved emitter designs fall in the first category⁽³⁾. Controlling the defect content and purity of the bulk material to increase diffusion length are important aspects of material quality. Impurity effects and their control are the subjects of this paper.

Mathematical models of the solar cell can be used effectively to analyze how parameters like carrier diffusion length control device performance, and how they can be manipulated to gain efficiency improvement. We have used two types of models to evaluate device performance and impurity effects: one-dimensional analytic models which relate the overall material and design parameters to cell efficiency^(4,5), and a semi-empirical impurity effects model which connects the concentration of specific impurities to diffusion length and cell performance⁽⁶⁾.

In the one-dimensional model, the solar cell is divided into several elements, and the surface recombination velocity (S_0), the base diffusion length, the cell width, and the doping density are input variables. The internal recombination velocity is calculated iteratively from the device surfaces toward the junction using the relation

$$S_2 = \frac{N_2}{N_1} \frac{D}{L} \exp(\Delta V_{G2} - \Delta V_{G1}) \frac{S_1 \frac{L}{D} + \tanh\left(\frac{W}{L}\right)}{1 + S_1 \frac{L}{D} \tanh\left(\frac{W}{L}\right)} \quad (2)$$

where W is the width of the element; $(S_1, N_1, \Delta V_{G1})$ and $(S_2, N_2, \Delta V_{G2})$ are the recombination velocity, doping density, and the bandgap narrowing at the two boundaries of the element. (Here D and L are the diffusivity and diffusion length of the minority carriers within the element.) With this approach V_{oc} is calculated which, when coupled with measured or estimated values of I_{sc} , gives the expected cell efficiency⁽⁴⁾.

Figure 1 for example, illustrates the internal recombination velocities calculated for a cell made from a 250 μm thick 4 Ωcm resistivity silicon having a base diffusion length of 400 μm and various degrees of surface passivation^(4,5).

Passivation of the front and back surfaces is assumed to reduce surface recombination rates from 10^6 to 500 cm/sec in the model with resultant reduced recombination throughout the device. For the passivated device in the figure, cell efficiency is increased from 15.2% to 17% by the passivation step alone, a prediction which has been experimentally verified⁽⁷⁾. Improvements to the model⁽⁵⁾ permit direct calculation of I_{sc} and finally the cell efficiency.

If we make no assumptions regarding the mechanisms limiting the bulk material quality, we can employ the one-dimensional model to estimate how changes in the base material properties affect cell performance. The key parameter is the carrier diffusion length. We want L to be comparable to, or larger than the cell thickness to maximize efficiency. Defects such as dislocations, grain boundaries, impurity-induced recombination centers and to some extent the doping concentration all affect the value of L .

High cell efficiency can be reached by different combinations of resistivity and diffusion length as illustrated by the calculations listed in Table 1. In these specific passivated devices ($S_{on}^+ = 500$, $S_{op}^+ = 500$ cm/sec), 17.5% efficient cells required a 467 μm diffusion length when the base doping level corresponded to 4 Ωcm , but only a 125 μm diffusion length when base resistivity was 0.2 Ωcm . Increases in V_{oc} more than offset the reduction in I_{sc} due to the shorter diffusion length in the low resistivity cells. If the diffusion length of the low resistivity material is raised to 300 μm (coupled with a reduction in emitter doping to $1 \times 10^{19} \text{ cm}^{-3}$), cell efficiencies over 20% are predicted.

The important point to recognize is that once cell design and resistivity are fixed, the base material diffusion length becomes the controlling parameter for efficiency improvement. Each doubling of minority carrier lifetime τ produces an absolute efficiency improvement of about 0.5%.

3. IMPURITY EFFECTS

3.1 Diffusion Length

Detailed analyses of impurities in silicon solar cells^(6,8) indicate that most metal impurities form carrier recombination centers in the bandgap and thus degrade solar cell performance dominantly by reducing diffusion length and device short circuit current. For example, Figure 2 depicts the energy levels of centers measured by deep level transient spectroscopy (DLTS) on silicon single crystals grown from melts purposely contaminated with impurities. The DLTS method is unique in its ability to detect minute amounts of active impurities⁽⁸⁾. The DLTS detection limit is about four orders of magnitude below the doping density, so concentrations as low as 10^{10} cm^{-3} (0.5 parts per trillion) can be detected in high resistivity silicon. Each impurity exhibits a particular energy level or levels which are characterized by an energy, a density, and a capture cross-section for holes or electrons.

By comparing the concentration of electrically-active (deep level) impurities in a crystal with the total metallurgical impurity content (determined by neutron activation analysis or mass spectroscopy), we discovered that the fraction of impurity that remains electrically active, and thus affects device performance, varies with the metal species, viz, Figure 3. For example all the Mo in a crystal is active following growth while only about 23% of the Cr atoms contribute to cell performance reduction. This is an indication that material thermal history strongly influences final cell efficiency, a point we will return to later.

The DLTS data on impurity recombination effects are supported by detailed dark IV measurements like those for Ti in Figure 4. The position of the upper segment of the IV curve directly relates to the bulk diffusion length of the base material^(6,9). The upward shift of the curve corresponds to an increase in I_0 , the current intercept at $V = 0$ indicating reduction in the bulk diffusion length^(6,10). The reduction in L correlates directly with the electrically active concentration (N_T) of impurities measured in the silicon by DLTS: $I_0 \propto \frac{1}{L} \propto \sqrt{N_T}$. Data for Ti were typical of most impurities studied; a few like Cu and Ni produce no apparent diffusion length reduction but degrade solar cell junctions by forming precipitates which act as electrical short circuits⁽⁶⁾.

3.2 Impurity Effects Model

The DLTS and dark IV analyses provide the foundation for an impurity effects model which gives a relationship between silicon impurity concentration and the conversion efficiency in high performance devices^(6,10). Briefly, the assumptions of the model are that the device performance is base controlled, that impurities primarily degrade diffusion length and that the number of recombination centers produced is a linear function of the metallurgical concentration of the contaminating species present.

From these assumptions, we showed that the bulk diffusion length is related to L_{no} , the diffusion length in the uncontaminated solar cell, by $\frac{1}{L^2} = \frac{1}{L_{no}^2} + K_x N_x + K_y N_y + \dots + K_z N_z$ where the K 's are constants and N is the metallurgical concentration of a given species⁽⁶⁾. For this case I_n , the

short circuit current of the contaminated devices normalized by the value for the metal-free baseline cells is given by

$$\left[\frac{I_{n\infty}}{I_n} - 1 \right]^2 = C_{2x} (N_{ox} + N_x) \quad (3)$$

in which $I_{n\infty}$ (a constant related to device geometry) = 1.11, N_x is the metallurgical impurity concentration and C_{2x} and N_{ox} are model constants determined by fitting the equation to experimental data^(6,10). N_{ox} can be interpreted as a threshold concentration for the onset of cell degradation; at $N_x = N_{ox}$, $I_n = 0.97$ and the normalized efficiency $\eta/\eta_0 = 0.92$.

We showed further that this equation can be coupled with an empirical approximation to the relationship between normalized efficiency and I_n so that cell efficiency as a function of impurity content is given by

$$\eta/\eta_0 = 0.8721 I_n^{1.128} + 0.1279 I_n^{12} \quad (4)$$

A least squares fit of equation (3) to the short circuit current data for Mo-doped cells yields $C_{2x} = 2.0 \times 10^{-14}$ and $N_{ox} = 6.08 \times 10^{11} \text{ cm}^{-3}$. The fit of the model to the efficiency data for Mo is illustrated in Figure 5. The threshold values obtained in similar fashion for over twenty metal impurities are tabulated in Reference 6. Figure 6 illustrates how the threshold for cell degradation, N_{ox} , varies with the position of the metal element in the periodic table. With these values of N_{ox} , equations (3) and (4) can be used to obtain the cell efficiency as a function of impurity type and content. The projected curves resemble Figure 5 and describe the experimentally observed behavior of 26 metals very well⁽⁶⁾ reinforcing the conclusion that the primary effect of the impurity is to degrade bulk lifetime by carrier recombination at a trapping center.

The model predicts well the behavior of both singly and multiply-contaminated solar cells made using either conventional diffused n^+ or p^+ junction designs lacking a back surface field, surface passivation, or other refinements. The average cell efficiency of this "standard efficiency" (SE) device made on silicon containing no purposely added contaminants was $14.1 \pm 0.7\%$ ^(6,10).

3.3 High Efficiency Cells

Using data for our conventional (SE) devices a qualitative understanding of how material properties influence the performance of cells with higher efficiencies can be attained by extension of the impurity effects model. A convenient way to do this is to determine the threshold impurity concentration N_{ox} for a higher efficiency (H) device and then to compare it to the value of N_{ox} deduced for our 4 Ωcm SE cells.

The relationship between the two types of devices was derived by Davis et al^(6,10):

$$N_{\text{ox}}(H) = N_{\text{ox}}(\text{SE}) \left[\frac{L_{\text{no}}(\text{SE})}{L_{\text{no}}(H)} \right]^2 \left(\frac{D_n(H)}{D_n(\text{SE})} \right) \quad (5)$$

$$\text{which reduces to } N_{\text{ox}}(H) = N_{\text{ox}}(\text{SE}) \left[\frac{L_{\text{no}}(\text{SE})}{L_{\text{no}}(H)} \right] \quad (6)$$

when both devices have the same base resistivity.

This relationship, plotted in Figure 7 for several impurities, indicates that the sensitivity of solar cells to impurities, measured by the degradation threshold, decreases as the quality of the material denoted by L_{no} increases. For example, raising L_{no} to 600 μm from 175 μm lowers the impurity concentration at which cell performance just begins to degrade to 2.2×10^{11} Ti atoms cm^{-3} from 2.5×10^{12} Ti atoms cm^{-3} . That is, as the performance of a device is increased by material quality improvements, the sensitivity of the device to trace contamination increases.

We can place this phenomena in the context of cell efficiency with the aid of Figure 8 in which the normalized solar cell efficiency is plotted versus Ti concentration for silicon base material whose uncontaminated diffusion lengths are 175, 450, and 600 μm , respectively. The baseline (uncontaminated) devices made using this SE design would have efficiencies of 14, 14.5, and 15%, respectively. In each case once the threshold value is exceeded the cell efficiency value falls monotonically with impurity concentration. However, for the higher efficiency devices the onset of efficiency reduction occurs at successingly lower Ti concentrations (lower N_{ox}) as forecast by equation (6).

With the addition of $2.6 \times 10^{12} \text{ cm}^{-3}$ of Ti, the efficiency of the device with $L_{\text{no}} = 175 \mu\text{m}$ would fall from 14% to 12.6% in absolute terms. The same relative efficiency reduction, 15% to 13.5% ($\eta/\eta_0 = 0.91$), would take place at a Ti concentration of only $2.2 \times 10^{11} \text{ cm}^{-3}$ in the device with $L_{\text{no}} = 600 \mu\text{m}$. Similar calculations can be made for other impurities using the values of N_{ox} for SE cells taken from Figure 6 or from Reference 6. Compared to Ti the onset of impurity degradation would occur at a lower concentration for impurities like Mo and at higher concentrations for impurities like Cr, viz Figure 6.

Sophisticated techniques like surface passivation, back surface fields, and special emitter designs should produce cell efficiencies of 20% or better, e.g., Table 1. To analyze impurity effects on these high efficiency (HE) designs, we need to make use of the more detailed one dimensional analytic model coupled with the established linkage between diffusion length and impurity content outlined above^(6,10). Using Ti as a typical impurity, we assume an HE device design with front and back surface passivation, a back surface field, a double layer antireflective coating and a cell thickness of 275 μm equal to that of the SE cells. Again, the assumed diffusion lengths of the uncontaminated baseline cells are 175, 450, and 600 μm , producing calculated cell efficiencies of 16.1, 18, and 18.5% AM1. As noted, the efficiency of the SE cell chosen for comparison is 14% when $L_{\text{no}} = 175 \mu\text{m}$.

The effect of Ti additions on HE cell performance, Figure 9, is qualitatively similar to that for the SE design: as the cell efficiency increases, the Ti concentration at which performance reduction begins is reduced. That is, higher efficiency devices are more impurity sensitive (quantitative comparisons of Figures 8 and 9 are difficult due to minor differences in the model assumptions for the two cases).

Taken together, the data indicate that small amounts of metal contaminants may be tolerated when cell efficiencies are low to moderate, 12 to 15%, but that impurities must be limited to very low levels if very high efficiencies are to be achieved (a Ti concentration of about 10^{11} cm^{-3} , 2 parts per trillion, is sufficient to reduce cell efficiency from 18.5% to about 16.8%). The harmfulness of a specific impurity depends on its value of N_{ox} , Figure 9. In addition, other defects which reduce bulk lifetime must also be minimized.

4. IMPURITY CONTROL

Currently there are two approaches to control the electrically-active impurity concentration in silicon solar cells: (1) minimize contamination of the base material by purification to provide the highest value of L possible in the wafers from which cells are made, and (2) maintain or improve the initial diffusion length by chemical or thermochemical "getting" techniques during the cell processing itself^(11,12). In the first method, impurities are eliminated; in the second, they may be removed or made electrically inactive by precipitation or chemical complexing to eliminate carrier recombination sites.

4.1 Purification

Silicon for solar cells is produced in two steps - decomposition of highly-purified trichlorosilane or silicon tetrachloride to form polycrystalline silicon⁽¹³⁾ and the subsequent transformation of polysilicon to a single crystal ingot by Czochralski pulling (CZ) or float zone (FZ) refining,^(14,15) or to sheet by newer ribbon growing processes⁽¹⁶⁾. The crystal growth step is an integral part of the purification since most impurities tend to accumulate preferentially in the liquid during growth leaving the solid proportionately purer. The degree of purification for a given contaminant is measured by its effective segregation coefficient k_e , the ratio of the crystal impurity content to the impurity content of the feedstock from which the crystal grew⁽¹⁵⁾.

Our measurements, Table 2, confirm that the segregation coefficients of metal contaminants grown into silicon crystals during Czochralski pulling^(6,10) are in general extremely small, ranging from 3×10^{-2} for Al to 1.7×10^{-8} for W. (k values for ribbon growing by the dendritic web process are comparably small⁽¹⁶⁾). Perhaps one of the most striking and useful features of metal impurity segregation in silicon is the relationship between the cell degradation threshold concentration and the effective segregation coefficient, viz Figure 10. Those impurities most effective at reducing bulk diffusion length, e.g., Ta, Mo, and Zr, have the smallest segregation coefficients and are therefore the most easy to eliminate during the crystal growth step.

Although there is no clear-cut theoretical explanation for the observed relationship, we expect impurities with the largest atom size and chemical character disparities to silicon to exhibit the smallest value of k , a fact consistent with experiment, viz Figure 11 (see also reference 10). These are the same impurities whose electronic structure favor the formation of deep levels with large carrier capture cross-sections⁽¹⁷⁾. The general sloping of the threshold values from the upper right to lower left in Figure 6 though not completely understood, suggests an increase in effective carrier recombination cross-section.

To take fullest advantage of the segregation behavior of metal contaminants, we can employ zone refining to purify the silicon from which cells are made. For example, after two zone passes our model Ti impurity could be reduced below 10^{10} cm^{-3} from an assumed feedstock concentration of 10^{16} cm^{-3} . The purification effect would be somewhat less for CZ pulling and web growth, but it is still significant. Experimentally, the most efficient solar cells have been produced on Wacker float zoned silicon substrates. Data for cells made in our laboratory on FZ material, Table 3, show the obvious advantages of increased purification. Comparable cells made on Czochralski and web material typically exhibited efficiencies lower by as much as 1 to 2% absolute. The purity of these materials is high enough that no deep levels can be measured even by DLTS; total heavy metal impurity concentrations of less than 0.01 ppba ($5 \times 10^{11} \text{ cm}^{-3}$) for float zone silicon and less than 1 ppba ($5 \times 10^{13} \text{ cm}^{-3}$) for Czochralski material are typical⁽¹²⁾.

4.2 Post Growth Impurity Control

Despite the fact that crystals of extremely high purity can be produced, contaminants introduced during subsequent device processing may significantly degrade bulk material properties. Wafer preparation, handling, and high temperature process steps are common entry points for metal species into the silicon⁽¹⁸⁾. Besides cleaner processing, one way to minimize the effects of contamination and to enhance bulk material properties is by impurity gettering^(11,12).

We found that volatilization of impurities as chlorides by heat treatment in Cl-bearing ambients, migration of contaminants to regions of enhanced solubility such as diffused junctions, and precipitation at deliberately induced defects all can be used to electrically deactivate impurities in silicon solar cells and to raise cell efficiency^(10,19). However, the effectiveness of each technique appears highly species and process history dependent.

A key step in most gettering processes is the diffusion of impurity atoms to a sink where the electrical activity of the metal is ultimately neutralized by precipitation or complexing. To test the response of various species to gettering, we diffused metal-doped wafers at 825°C in POCl_3 , a treatment which also mimics the solar cell junction formation step. The diffused layer was dissolved, and a series of steps was etched from the wafer surface into the bulk silicon. Schottky diodes formed on the steps permitted us to measure by DLTS the impurity concentration as a function of depth into the wafer, Figure 12. The starting wafer concentrations were $4 \times 10^{14} \text{ cm}^{-3}$ V, $2 \times 10^{14} \text{ cm}^{-3}$ Ti, 10^{15} cm^{-3} Cr, and $4 \times 10^{12} \text{ cm}^{-3}$ Mo, respectively.

The variation in impurity response to the thermochemical process is striking. Following gettering, the electrically active Ti and V concentrations exhibited a profile with decreasing concentration toward the surface indicating diffusion of the metals to the junction region and electrical deactivation. The electrically active Cr concentration which was about 10^{14} before heat treatment fell below the DLTS detection limit of $3.5 \times 10^{11} \text{ cm}^{-3}$ at all locations in the sample. No change in the Mo concentration could be detected. A more detailed study of Ti gettering, Figure 13, indicated that the process was diffusion controlled and could be modeled closely by assuming an activation energy of 1.66 eV⁽¹³⁾. In general, the effectiveness of POCl_3 gettering depended directly on the diffusion coefficient of the species ($D_{\text{Cr}} > D_{\text{Ti}} > D_{\text{V}} > D_{\text{Mo}}$) and so the process cycle must be tailored to some extent for each impurity or class of impurity (Fe, Cr, Co, Cu).

For example, the data in Table 4 indicate how solar cell efficiency and silicon impurity concentration vary with the gettering treatment for silicon which initially contained $8 \times 10^{13} \text{ cm}^{-3}$ of electrically active Ti. Higher temperatures and longer times decrease the Ti concentration near the surface and increase the cell efficiency. For the starting concentration chosen in these experiments, no process tested completely deactivated all the Ti, so the cell efficiency recovered to only about 70% of the uncontaminated baseline value of 14%. For rapidly diffusing species like Cr and Fe, full recovery of the baseline cell efficiency was achieved^(10,19). For impurities like Mo, almost no improvement in cell efficiency was obtained even after several hours POCl_3 gettering at 1200°C.

HCl treatments at temperatures between 825 and 1200°C provided qualitatively similar results but appeared to be somewhat more effective than the POCl_3 treatment. Shorter times or lower temperatures diminished the impurity effects to the same level as for POCl_3 . Backside damage and argon implant-induced damage reduced the electrical activity of most contaminants studied but were most effective when used in combination with HCl treatments⁽¹⁰⁾.

The data on gettering are encouraging as a means to improve cell efficiency, but we know of no systematic studies in which the method has been employed to produce higher efficiency devices than those attained by conventional methods.

Coupled with float zoning, gettering may provide material quality enhancements permitting the full exploitation of device design improvements suggested from the model studies.

5. CONCLUSION

Economic analyses indicate that high efficiency (> 18%) solar cells and modules will be required if photovoltaic power generation systems are to achieve widespread application, especially in utility networks. While clever cell design can produce significant efficiency improvements, the quality of the silicon from which the cells are made must be increased and its bulk properties maintained during cell processing if these design improvements are to be fully realized.

Cell efficiency, particularly in high efficiency devices, is strongly degraded by metal contaminants which reduce bulk diffusion length. For example, as few as 10^{11} cm^{-3} Ti atoms cm^{-3} can reduce the efficiency of an 18.5% to 16.8%, a significant depreciation. Elements to the left of the periodic table like W and Mo are more harmful per unit concentration than are elements to the right like Cr and Fe. Low base resistivity permits lower diffusion lengths for a given efficiency so that such devices are more impurity tolerant.

Raising bulk diffusion length can be achieved mainly by starting with high purity silicon then employing zone refining. The segregation coefficients for all metal contaminants are small, typically 10^{-5} or less so that several zone passes lower the impurity concentration well below the detection limits of even the most sensitive analytical techniques. To preserve diffusion length during silicon handling is more difficult and requires extremely clean procedures to guard against unwanted contamination. A gettering step to maintain diffusion length during processing ultimately may be required to provide the highest efficiency devices.

ACKNOWLEDGEMENTS

We acknowledge the major contributions to this work by our colleagues at the Westinghouse R&D Center and Advanced Energy Systems Division including the late J. R. Davis, D. L. Meier, P. G. McMullin, M. H. Hanes, P. D. Blais, P. Rai-Choudhury, R. G. Seidensticker, and R. B. Campbell. We also thank Dr. Martin Wolf, U. of Pennsylvania for use of the program SPCOLAY to model solar cell performance.

The work was supported by the DOE/JPL Flat Plate Solar Array Project.

REFERENCES

1. A. Rohatgi and E. F. Federman, J. Solar Energy (1985).
2. D. L. Bowler and M. Wolf, IEEE Transactions Compon. Hybrid Manufact. Tech., V3, p. 464, (1980).
3. M. Wolf, Proc. 14th IEEE Photovoltaic Specialists Conference, p. 674, (1980).
4. J. R. Davis and A. Rohatgi, Proceedings 14th IEEE Photovoltaic Specialists Conference, p. 569 (1980).
5. M. Wolf, IEEE Transactions on Electron Devices, V ED-28, p. 566, (1981).
6. J. R. Davis et al, IEEE Transaction on Electron Devices, V ED-27, p. 677, (1980).
7. A. Rohatgi and P. Rai-Choudhury, IEEE Transactions on Electron Devices, ED-31, p. 596 (1984).
8. A. Rohatgi, J. R. Davis, R. H. Hopkins, and P. G. McMullin, Solid State Electronics, V26, pl. 1039, (1983).
9. A. Rohatgi, R. H. Hopkins, J. R. Davis, and R. B. Campbell, Solid State Electronics, V. 23, p. 1185, (1980).
10. R. H. Hopkins et al, Final Report, Impurity Effects in Silicon Solar Cells, DOE/JPL 954331, (1982).
11. L. E. Katz, P. F. Schmidt, and C. W. Pearce, J. Electrochem. Soc., V 128, p. 620, (1981).
12. J. R. Monkowski, Solid State Technology, p. 44 (1981).
13. See e.g., J. Dietl, D. Helmreich, and E. Sirtl, Crystals: Growth Properties and Applications, V 5, p. 43, (1981).
14. W. Zulehner and D. Huber, Crystals: Growth Properties and Applications, V 8, p. 3, (1982).
15. B. Chalmers, Principles of Solidification (J. Wiley & Sons, NY), p. 3, (1964).
16. R. G. Seidensticker, Crystals: Growth, Properties and Applications, V 8, p. (1982).
17. L. A. Hemstreet, Phys. Rev. B, V 15, p. 834 (1977).
18. P. F. Schmidt and C. W. Pearce, J. Electrochem Soc., V 128, p. 630 (1981).
19. A. Rohatgi et al., Proceedings 14th IEEE Photovoltaic Specialists Conf., p. 908, (1980).

LIST OF FIGURES

1. Model Calculations and Internal Recombination Velocity Plots for 4-ohm-cm Base Cells with a Base Diffusion Length of 400.
2. Measured Deep Levels for Impurities Grown into Silicon Single Crystals.
3. Measured Electrically Active Deep-Level Concentrations versus the Metallurgical Concentrations for Several Metal Impurities.
4. Transferred Dark IV Curves for Ti-Doped Solar Cells.
5. Calculated and Measured Cell Performance for Mo-Contaminated Devices.
6. Threshold Impurity Concentrations for Cell Performance Reduction.
7. Variation in Degradation Threshold with Diffusion Length of Baseline SE Cell.
8. Cell Efficiency Variation with Ti Concentration for Various Initial Base Diffusion Lengths.
9. Variation in Cell Performance with Ti Concentration: HE Cell Design.
10. Relation of Cell Degradation Threshold to Impurity Segregation Coefficient.
11. Variation of Segregation Coefficient with Impurity Bond Radius.
12. Electrically Active Impurity Profiles for Several Species after an 825°C, 50-min POCl_3 Treatment.
13. Electrically Active Ti Concentration Profiles Following 50-min POCl_3 Gettering at Several Temperatures.

TABLE 1

RESISTIVITY AND DIFFUSION LENGTH REOUIREMENTS
FOR HIGH EFFICIENCY SOLAR CELLS

$W = 150 \text{ } \mu\text{m}$ (cell thickness)

$N_{xj} = 3 \times 10^{17} \text{ cm}^{-3}$ (emitter junction edge doping concentration)

$S_{op}^+ = S_{on}^+ = 500 \text{ cm/sec}$ (surface recombination velocities)

$N_s = 2 \times 10^{20} \text{ cm}^{-3}$ (emitter surface coping concentration)

ρ <u>$\Omega\text{-cm}$</u>	L <u>(μm)</u>	J_{sc} <u>(ma/cm^2)</u>	V_{oc} <u>(volts)</u>	η <u>$(\%)$</u>
4.0	467	35.2	.597	17.5
0.2	125	33.2	.634	17.5
*0.2	300	35.0	.687	20.3

$$*N_s = 1 \times 10^{19} \text{ cm}^{-3}$$

TABLE 2

EFFECTIVE SEGREGATION COEFFICIENTS IN SILICON

<u>Element</u>	<u>Segregation Coefficient</u>
Ag	1.7×10^{-5}
Al	3×10^{-2}
Au	2.5×10^{-5}
Co	2×10^{-5}
Cr	1.1×10^{-5}
Cu	8.0×10^{-4}
Fe	6.4×10^{-6}
Mn	1.3×10^{-5}
Mo	4.5×10^{-8}
Nb	4.4×10^{-7}
Ni	1.3×10^{-4}
Pd	5×10^{-5}
Sn	3.2×10^{-2}
Ta	2.1×10^{-8}
Ti	2.0×10^{-6}
V	4×10^{-6}
W	1.7×10^{-8}
Zr	1.6×10^{-8}

TABLE 3

OXIDE-PASSIVATED SOLAR CELLS WITH DOUBLE-LAYER ANTIREFLECTIVE
COATING PRODUCED ON 0.25 Ω -cm FLOAT ZONED SILICON

<u>Cell ID*</u>	<u>Area cm²</u>	<u>J_{sc} mA/cm²</u>	<u>V_{oc} mV</u>	<u>FF</u>	<u>η %</u>
25-1	1.0	37.5	614	0.791	18.2
25-2	1.0	37.1	617	0.784	18.0
9-1	1.0	36.8	617	0.797	18.1
9-2	1.0	36.3	617	0.806	18.0
4-1	1.0	35.9	623	0.809	18.1
4-2	1.0	36.2	622	0.809	18.2
4-3	1.0	36.1	623	0.815	18.3
4-4	1.0	36.0	622	0.809	18.1

TABLE 4

VARIATION IN CELL EFFICIENCY AND TRAP CONCENTRATION (N_T) AS A FUNCTION OF
GETTERING TREATMENT FOR SILICON CONTAINING A METALLURGICAL TI

<u>Gettering Condition</u>	<u>Cell Efficiency (%)</u>	<u>Concentration (N_T) of $E_V + 0.30$ eV TRAP (cm⁻³)</u>
None (starting wafer)	---	8.0×10^{13}
None (solar cell)	5.88	1.76×10^{13}
950°C/1 hr.	6.58	6.35×10^{12}
1000°C/1 hr.	7.14	3.94×10^{12}
1100°C/1 hr.	7.42	2.99×10^{12}
1100°C/2 hr.	7.76	2.50×10^{12}
1100°C/3 hr.	8.27	2.39×10^{12}
1100°C/5 hr.	9.27	1.49×10^{12}

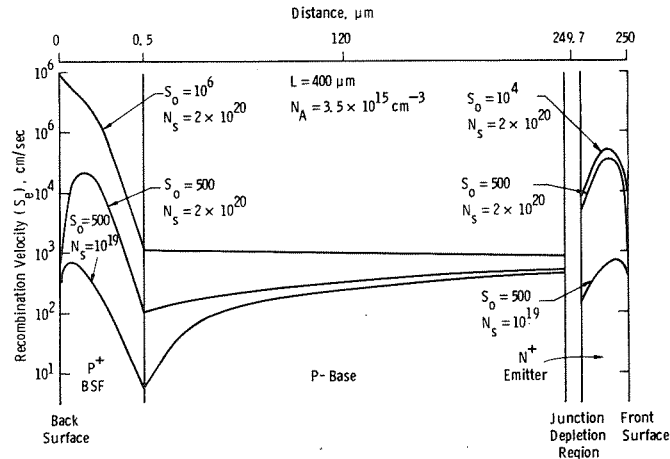


Figure 1 Model Calculations and Internal Recombination Velocity Plots for 4-ohm-cm Base Cells with a Base Diffusion Length of 400 μm

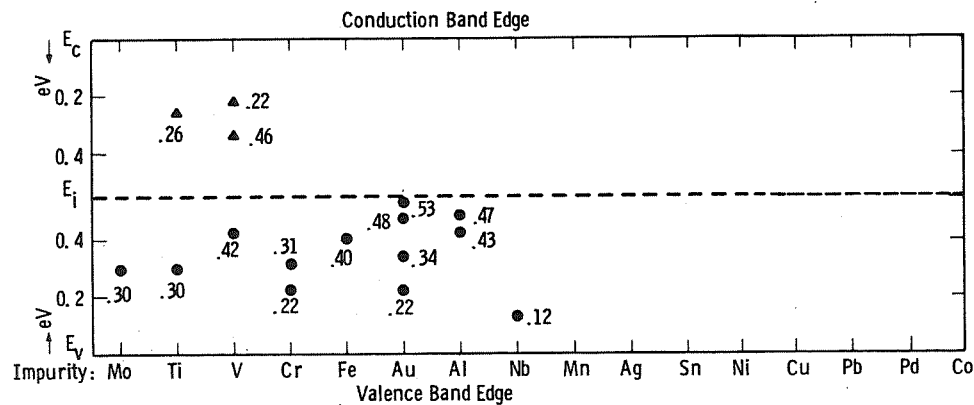


Figure 2 Measured Deep Levels for Impurities Grown into Silicon Single Crystals.

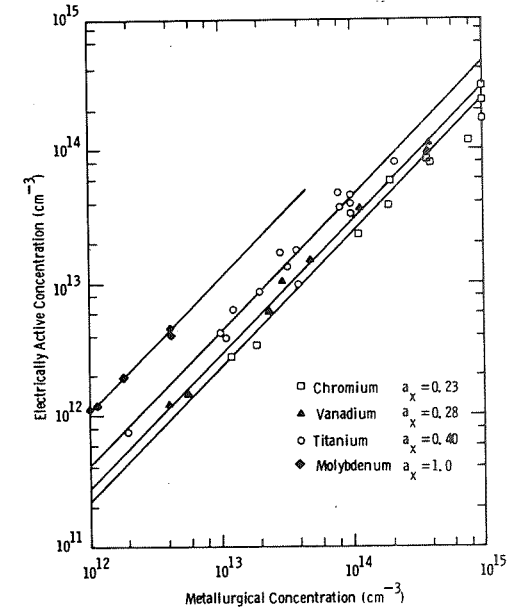


Figure 3 Measured Electrically Active Deep-Level Concentrations versus the Metallurgical Concentrations for Several Metal Impurities.

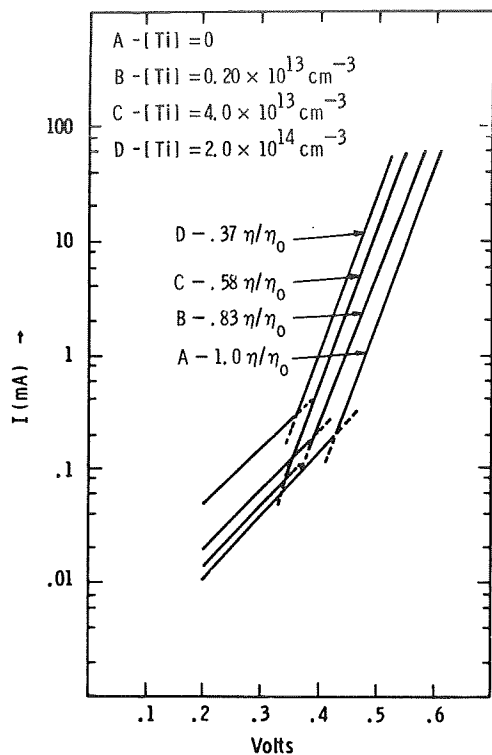


Figure 4 Transformed Dark IV Curves for Ti-Doped Solar Cells.

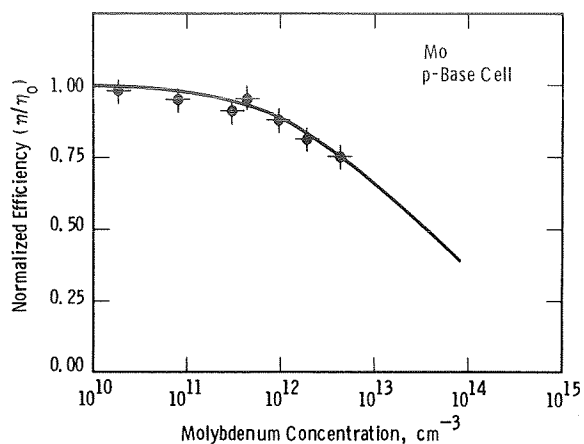


Figure 5 Calculated and Measured Cell Performance for Mo-Contaminated Devices.

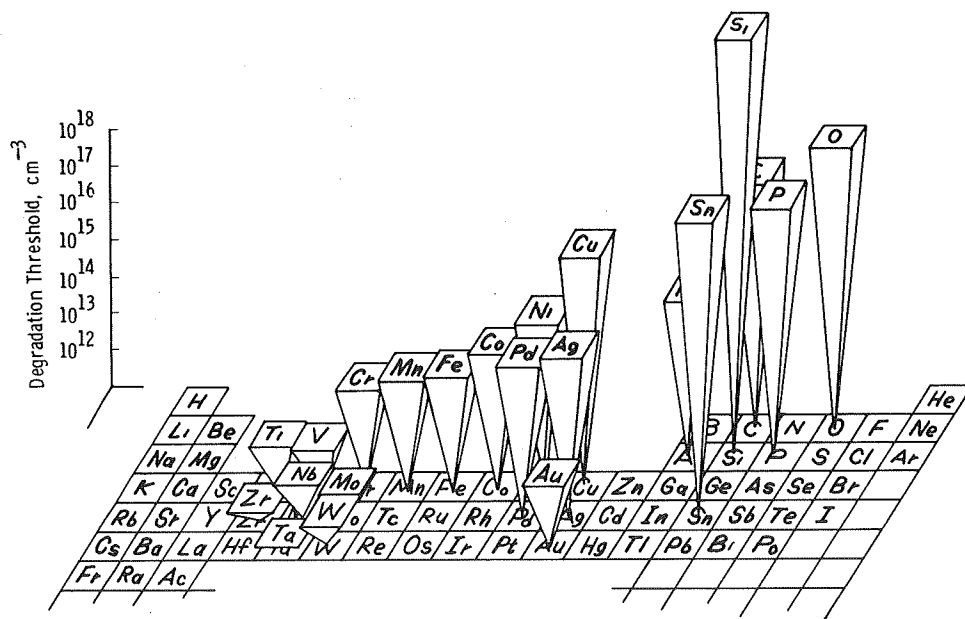


Figure 6 Threshold Impurity Concentrations for Cell Performance Reduction.

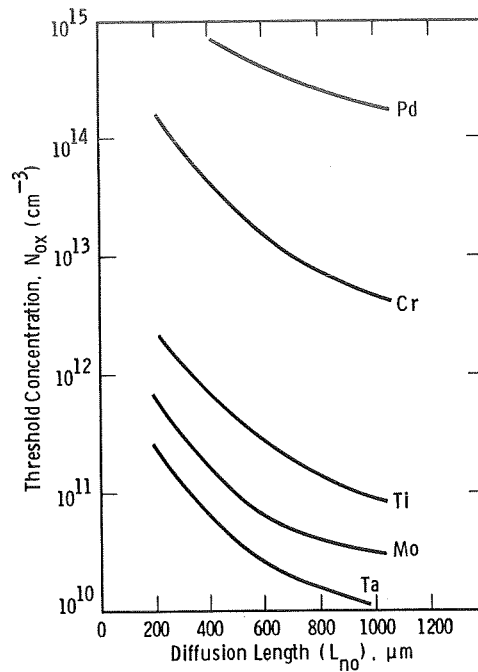


Figure 7 Variation in Degradation Threshold with Diffusion Length of Baseline SE Cell.

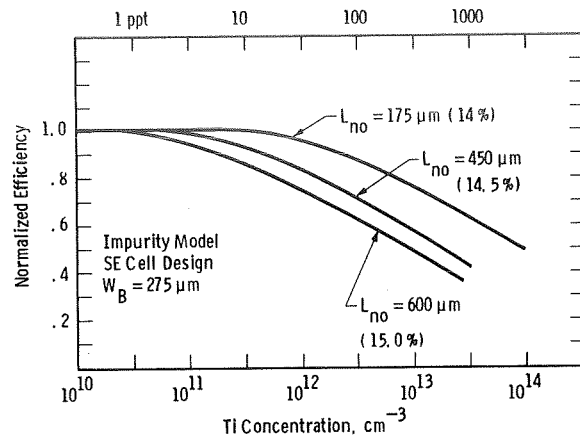


Figure 8 Cell Efficiency Variation with Ti Concentration for Various Initial Base Diffusion Lengths.

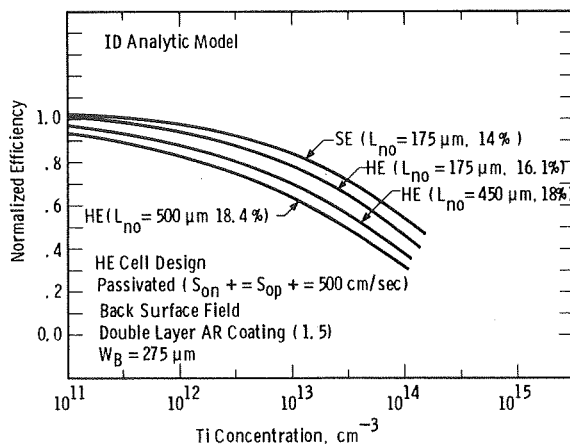


Figure 9 Variation in Cell Performance with Ti Concentration: HE Cell Design.

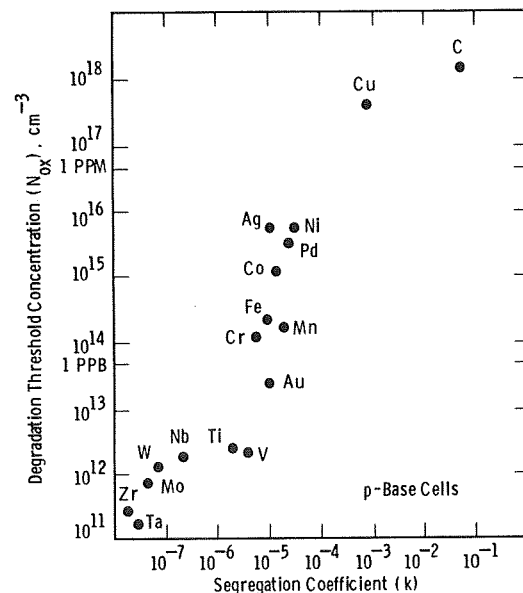


Figure 10 Relation of Cell Degradation Threshold to Impurity Segregation Coefficient.

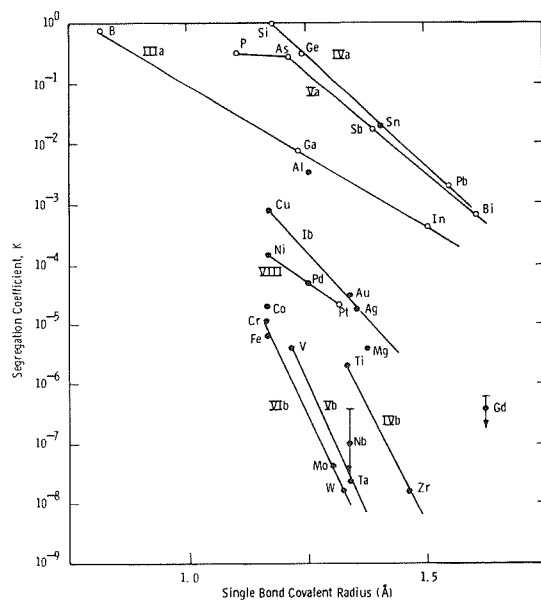


Figure 11 Variation of Segregation Coefficient with Impurity Bond Radius.

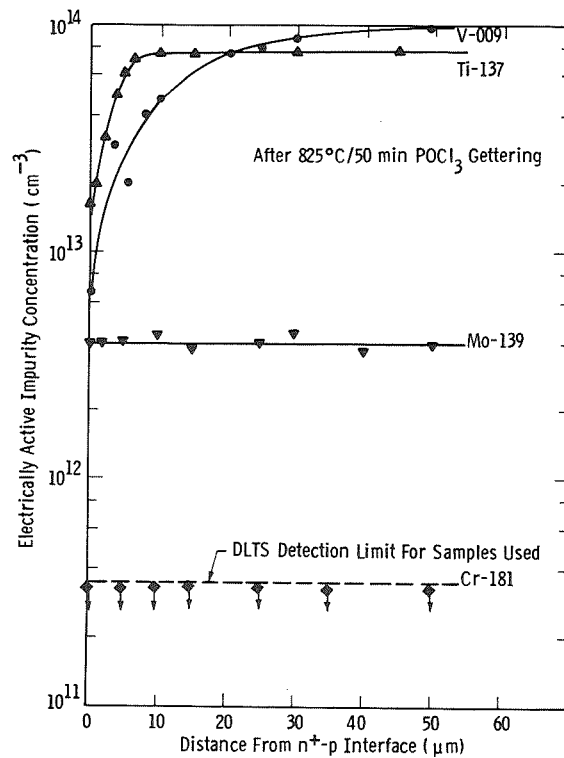


Figure 12 Electrically Active Impurity Profiles for Several Species after an 825°C, 50-min POCl_3 Treatment.

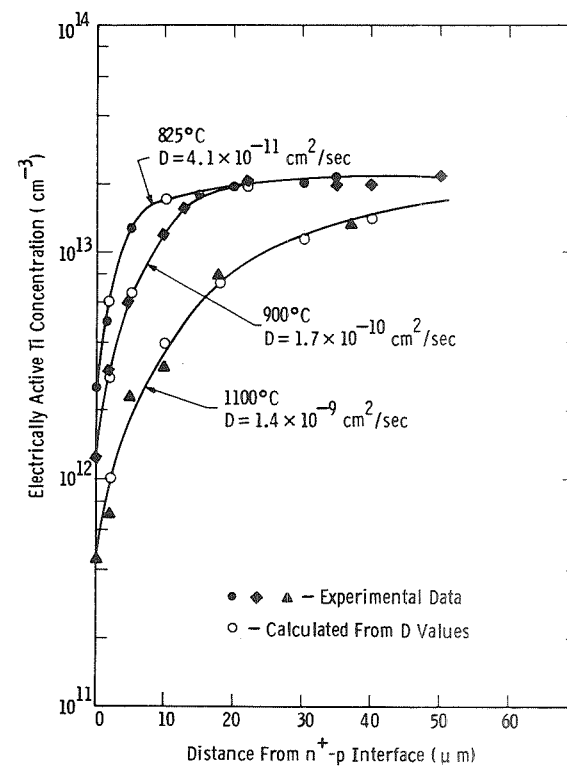


Figure 13 Electrically Active Ti Concentration Profiles Following 50-min POCl_3 Gettering at Several Temperatures.

omit

DISCUSSION

AULICH: Did you look at the effects of boron, phosphorus, and carbon on the impurity relationships?

HOPKINS: We did a very small amount of work with carbon. We had a great deal of difficulty getting structurally good ingots. Jim McCormick (Hemlock Semiconductor) is more familiar with the ingot-growing problems and could answer questions about that part better than I can. We really didn't investigate carbon extensively. We did some work with phosphorus. I can't remember the concentration levels, but they were fairly high. There does seem to be a turnover for phosphorus. Ranny Davis believed that this was largely due to a reduction in mobility due to ionized impurity scattering. We did not do a significant study using boron.

AULICH: If an impurity level is detrimental, can anything be done during cell processing to inactivate the impurity? In other words, is there a chance of converting an impure, bad material into a good efficiency material?

HOPKINS: Our experience wouldn't lead to a claim that this could be done. However, in some of our systematic studies of gettering using conventional back-surface damage (or phosphorus oxychloride or HCL as gettering agents, or in some cases using ion implantation damage to stimulate gettering), we found that the electrically active concentrations of a number of the impurities could be deactivated or reduced. If the impurities behaved like chromium and iron, which have relatively high diffusion coefficients, the electrically active concentrations were reduced to essentially zero. The concentrations of impurities having diffusion properties similar to titanium and vanadium could be reduced, but not eliminated. Thus, the efficiencies of devices containing titanium or vanadium, for example, could be improved by one or maybe two points over the range of temperatures and times we used experimentally, but the uncontaminated baseline values could not be reached. Some benefits can be obtained from gettering. We didn't do enough to really define the total spectrum of conditions needed to render all impurities harmless, but I think there is a limit to how much can be done if the initial impurity concentrations are very high.

HWANG: In a recent report describing silicon solar cells with efficiencies exceeding 18%, the materials used (with very few exceptions) were float-zone crystals with resistivities of 0.2 to 0.3 ohm-cm. This seems to indicate that phosphorus and boron might have a larger effect than the metal content. In these cases, the diffusion lengths were just a few tenths of a micrometer. Would you kindly comment on these data?

HOPKINS: What you said is true. In fact, the data that I showed for the 18% cells were for cells made from a seemingly unique piece of low-resistivity float-zone material. It doesn't seem to be unique anymore. The diffusion length was low, but it was still up in the hundreds of micrometers. I think the metal contamination levels must be kept very low to achieve these high-efficiency values. In fact, in our modeling of the 18%

devices, it became clear that the diffusion length must be high, which it was, even though the resistivity was low. Our conclusion was that the impurity concentrations must be kept at very low levels to get high-efficiency cells.

SCHMID: It seems that oxygen and carbon would be very significant elements in influencing the levels of impurities. I guess most of the work you did was with high-quality silicon. What were the levels of oxygen and carbon?

HOPKINS: Levels of oxygen were typically those found in most Czochralski-grown ingots, on the order of 10^{18} , and the level of carbon was about an order of magnitude lower. We did some work with float-zone crystals, and we found that the oxygen and carbon were reduced and there were lower levels of the metal impurities, although it wasn't dramatic. However, we only looked at three or four ingots out of a total of 200 or more.

SCHMID: You mentioned that you did some work in higher carbon content and you did see some breakdown. At what level did you see the breakdown as a factor of just increasing carbon concentration?

HOPKINS: I wish I could answer. It's been quite awhile, and the amount of work we did with carbon was relatively low. I don't think I can characterize the effects. I think the people who work with castings could describe the levels of carbon concentration which cause problems. As I said, we used Czochralski ingots for most of our work, and the main issue was to maintain the oxygen and carbon concentrations nearly the same from crystal to crystal to provide a valid method of comparison for determining the effects of impurities. I would like to look at that problem. If our program had not ended in 1982, we would have.